RAPID COMMUNICATIONS

PHYSICAL REVIEW B VOLUME 52, NUMBER 16 15 OCTOBER 1995-II

Completion of the structural determination of and rationalization of the surface-structure sequence (2×1)→(3×3)→(4×4) formed on Cu(001) with increasing Li coverage

Seigi Mizuno and Hiroshi Tochihara*
Catalysis Research Center, Hokkaido University, Kita-ku, Sapporo 060, Japan

Angelo Barbieri† and Michel A. Van Hove
Materials Sciences Division, Lawrence Berkeley Laboratory, University of California, Berkeley, California 94720
(Received 7 August 1995)

With increasing Li coverage, the surface structure of Cu(001) evolves as (2×1)→(3×3)→(4×4) at room temperature. We here report the detailed structure of the most complex (4×4) phase determined by a dynamical low-energy electron diffraction (LEED) analysis with symmetrized automated tensor LEED. This completes the solution of these structures and allows a rationalization of their formation. The unit cell of the (4×4) structure consists of four Li adatoms forming a square cluster located on top of islands of nine Cu atoms; the islands are separated and joined by rows of substituting Li atoms.

Recent studies have revealed that alkali-metal adsorption on Cu, Al, and Au planes at room temperature leads to formation of complex surface structures involving considerable restructing of substrate atoms, as determined by low-energy electron diffraction (LEED), density functional theory, and scanning tunneling microscopy (STM). These structures are (3×3) for Li/Cu(001),[1] (2×2) for Li/Cu(111),[2] (2×2) for Na/Al(111),[3–5] $c(2\times2)$ for K/Au(110),[6,7] and $(1.08\sqrt{3}\times1.08\sqrt{3})R30°$ for Na/Au(111).[8] These are referred to as ordered surface alloys, and it is clear that structure determination is essential for their understanding. In particular, the systems Li/Cu(001) and Na/Al(111) exhibit sequential changes of surface structures with increasing alkali-metal coverages: (2×1) (Ref. 9) →(3×3)→(4×4) for Cu(001) (Ref. 10) and $(\sqrt{3}\times\sqrt{3})R30°$ (Ref. 11) →(2×2) →$(2\sqrt{3}\times2\sqrt{3})R30°$ for Al(111).[12] The structures at lower coverages in both systems have already been determined, while both higher-coverage ones have not been analyzed yet.

In the present paper we report the determination of the relatively quite complex (4×4) structure formed on Cu(001) by Li deposition at 300 K, by means of a symmetrized automated tensor LEED analysis. As mentioned above, the (4×4) follows the (2×1) and (3×3), which have already been determined. The (2×1) consists of a missing-row-type restructuring of the top Cu layer with substituting Li atoms being located in the missing-row sites.[9] The (3×3) consists of small pyramids of four Cu atoms capped by single Li atoms, the pyramids being separated and joined by pairs of substituting Li atoms.[1] The purpose of the present study is to determine the nature of the (4×4) structure and thereby to understand the reasons for the formation of this series of complex surface structures for Li/Cu(001).

The apparatus and experimental procedures are the same as in the previous studies.[1,2,9,10] Briefly, Li atoms were deposited onto Cu(001) from a SAES dispenser at 300 K and intensity-voltage (I-V) curves were measured at 180 K. The Li coverage, the ratio of the number density of Li adatoms to that of Cu atoms in the ideal top layer of Cu(001), was estimated by comparing LEED patterns at low and at room temperatures, and from Li KVV Auger intensities.[10] I-V curves were taken at normal incidence with an energy range from 20 to 200 eV on a 1-eV grid. The cumulative energy range over the 13 symmetrically inequivalent beams is 984 eV.

Our symmetrized automated tensor LEED program[13] was used to calculate I-V curves for (4×4) structure models. Initially, six phase shifts were used to represent atomic scattering ($l_{max}=5$), while the final structural refinement utilized seven phase shifts ($l_{max}=6$). The real part of the inner potential was determined during the course of the theory-experiment fit. The damping was represented by an imaginary part of the potential of −5.0 eV. We used 335 and 480 K for the Cu and Li Debye temperatures, respectively.[14]

A total of 24 structural models, shown in Fig. 1, were examined in detail in an initial survey for Cu(001)-(4×4)-Li in the present study. All models are selected under the condition that every atom is located on a fourfold hollow site and keeps the symmetry $p4mm$. In addition, the possible range of Li coverage is limited to $\frac{9}{16}$, $\frac{10}{16}$, or $\frac{11}{16}$ from previous studies.[10] [Note that the coverage of the (3×3) preceding the (4×4) is determine definitely to be $\frac{5}{9}$ in Ref. 1.] Briefly, models 1–8 correspond to Li overlayers. Models 9–16 are intermixed Cu-Li layers. Models 17–24 correspond to double layers consisting of an intermixed layer and a Li adlayer (except for model 23). The automated search algorithm was directed by minimizing the Pendry R factor, R_P (Ref. 15). Relaxation in the first complete Cu(001) layer and below is not allowed in the initial survey, and the number of structural parameters is given in parentheses in Fig. 1. In order to decrease the number of structural parameters entering the theory-experiment fit, we only allowed displacements of Li and Cu atoms preserving the $p4mm$ symmetry.

The R_P value of each model is indicated in Fig. 2. Model 18 gives the best fit of $R_P=0.217$, and model 19 gives the next best fit of $R_P=0.221$. They have similar structures and this supports that one of them is correct. Their common features are four Li adatoms on an island of nine Cu atoms surrounded by substituting Li atoms. We conclude that model 18 is best by further optimization of all symmetry-allowed

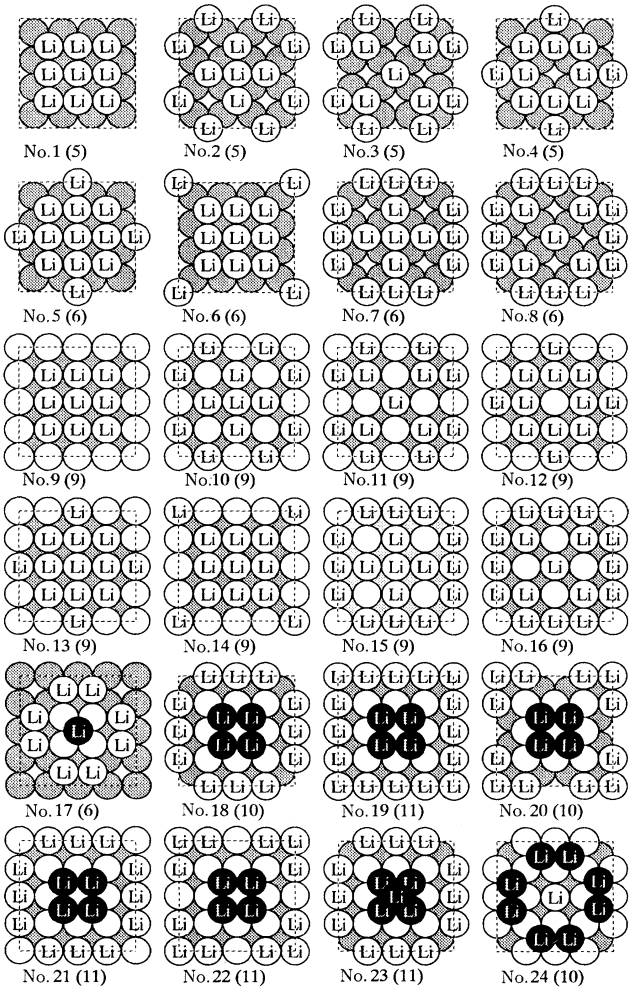

FIG. 1. Top views of 24 examined models for the Cu(001)-(4×4)-Li structure. Light-gray spheres represent Cu atoms in the first complete Cu layer, blank spheres are Cu or Li atoms in the mixed layer, while dark-gray spheres are Li adatoms in the adatom layer. All Li atoms are indicated as "Li." The dashed square indicates a (4×4) unit cell.

structural parameters in the first complete Cu layer and by use of $l_{max}=6$. The resulting R_P values are 0.175 and 0.195 for models 18 and 19, respectively.

In Fig. 3 the final optimized structure is shown: the directions of lateral displacements of inequivalent atoms are indicated by arrows and their values are listed in Table I. The second complete Cu(001) plane (shown as a line AA' in Fig. 3(b)] is used as a reference plane for atomic heights listed in Table I. The error bars were obtained from the variance of the R_P factor.[16] Note that due to the limited experimental database size, our lateral displacements are smaller than the error bars. In Fig. 4 the calculated I-V curves of the best-fit structure are compared with the experimental ones for the 13 beams. Agreement between theory and experiment is quite good for such a complex structure. We note that recent STM observation supports model 18.[17]

The best-fit Cu(001)-(4×4)-10Li structure [with ten Li atoms per (4×4) unit cell] has strong similarities with the

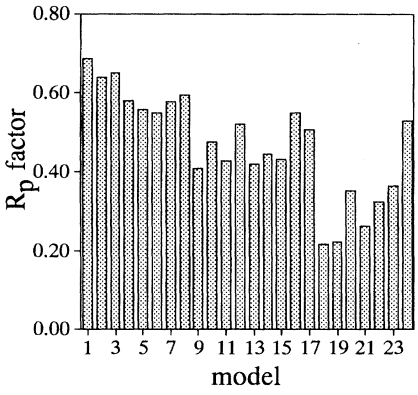

FIG. 2. R_P factor plotted against model number shown in Fig. 1.

Cu(001)-(3×3)-5Li structure: they both have Li adatoms on small Cu islands surrounded by substitutional Li atoms [the (3×3) structure looks very much like model 17 of Fig. 1, but fitted within a (3×3) cell]. The main difference is the increased size of these overlying Li groups (from one to four atoms), of the Cu islands (from four to nine atoms), and of the rows of substitutional Li atoms (from two to three atoms), to fit the larger unit cell. We emphasize some aspects of the best-fit structure (see Fig. 3 and Table I) in comparison with the (3×3) (see Ref. 1). The four Li1 adatoms (numbered 1 in Fig. 3) on a Cu island form a square cluster. The nearest-neighbor Li1-Li1 distance is 2.81 Å, while that of bulk Li metal is 3.02 Å. This short distance is consistent with

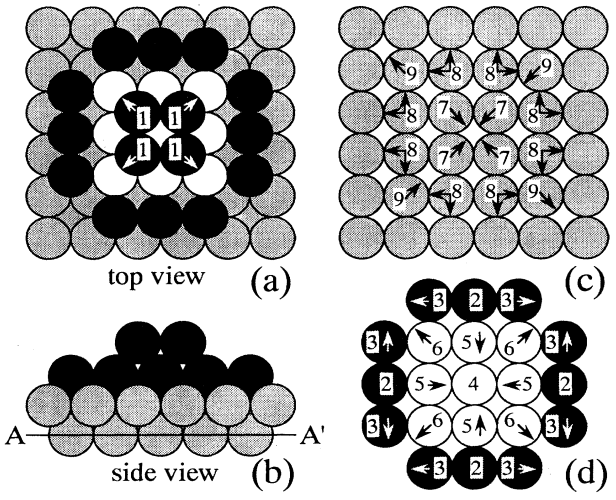

FIG. 3. (a) Top and (b) side views of the best-fit Cu(001)-(4×4)-10Li structure (model 18 in Fig. 1). Dark-gray spheres are Li atoms, light-gray spheres represent Cu atoms in the complete Cu layers, while blank spheres are Cu atoms in the mixed layer. The numbers identify symmetrically equivalent atoms. Arrows indicate directions of displacements from ideal hollow sites. The line A-A' in the side view is the base line for heights shown in Table I. (c) Top view of the first complete Cu(001) layer. (d) Top view of the mixed layer.

TABLE I. Optimum parameters of the best-fit structure for Cu(001)-(4×4)-10Li illustrated in Fig. 3. "No." identifies inequivalent atoms numbered in Fig. 3. "Lateral displacements" refer to displacements from the centers of hollow sites. Heights are measured from the plane A-A' in Fig. 3(b).

No.	Lateral displacement (Å)	Height (Å)
1	0.19±0.28	5.40±0.06
2		3.92±0.16
3	0.23±0.33	3.82±0.12
4		3.70±0.11
5	0.03±0.22	3.47±0.07
6	0.13±0.20	3.39±0.07
7	0.00±0.19	1.70±0.09
8	0.03±0.15, 0.02±0.15	1.77±0.06
9	0.03±0.25	1.74±0.08

the smaller number of bonding neighbors compared to the bulk, as expressed, e.g., in Pauling's bond-length rules.[18] While the lateral displacements are found to be smaller than our error bars, their optimized values are very suggestive of generally larger Li-Li distances compared to Cu-Cu distances, as one expects from bulk Li vs bulk Cu (3.02 vs 2.55 Å), as long as Li is assumed to remain rather metallic: with Li1-Li1 larger than bulk Cu-Cu, Li1 pushes Cu6 away from Cu4; Li2-Li3 is larger than the underlying Cu-Cu; Li2 pushes Cu5 toward Cu4, which thus buckles up, also because it is pulled up by the four Li1 atoms. Comparing with the (3×3) case, the height of the Li adatoms above the Cu island (average height of the Cu4, Cu5, and Cu6 atoms) is 1.88 Å, which is almost the same as the corresponding height for the (3×3), 1.91 Å. The distance between the substituting Li2 and Li3 is 2.78 Å, whereas the corresponding value for the (3×3) is 3.15 Å. This suggests that a considerably wide range of Li-Li distances is allowed in the missing-row sites. The substituting Li atoms are coordinated with six Cu atoms; four in the underlying Cu layer and two in the Cu islands, as in the (3×3) case. The average height of the Cu islands over the first complete layer of Cu(001) is larger (1.78 Å; cf. bulk value of 1.805 Å) in the (4×4) case than in the (3×3) case, where it is 1.67 Å. This may be due to the fact that the concentration of the missing rows is considerably decreased in the (4×4).

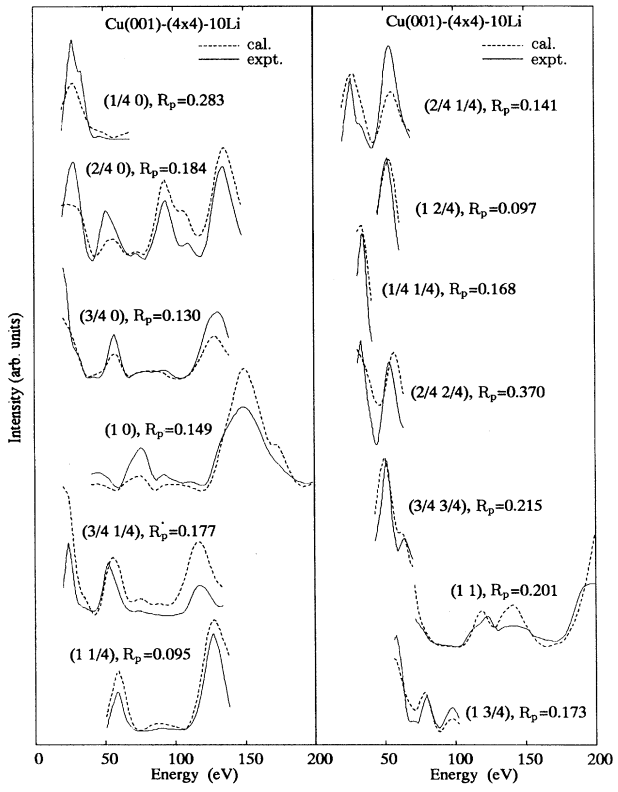

FIG. 4. Comparison between experimental (solid) and best-fit theoretical (dotted) I-V curves for the Cu(001)-(4×4)-10Li structure. The beam-specific value of the R_P factor is indicated by each I-V curve.

One may wonder why model 17 is not formed, since it is essentially the model found for the (3×3) case. Model 17 with a (4×4) cell is, however, energetically much less favorable than model 18, because the substitutional Li atoms have on average a lower coordination to Cu atoms in model 17. Since, in general, the binding energy between alkali-metal and substrate (such as Cu) atoms is much larger than that between alkali-metal atoms, higher coordination of Li to Cu atoms gives larger adsorption energy. Also, more vacancies exist in model 17. Model 19 has fewer vacancies, but the larger Li atoms cannot fit so tightly in the substitutional rows. Further comparison between the models of Fig. 1 would require total-energy calculations. However, it is instructive to compare the (2×1), (3×3), and (4×4) structures to gain a feeling for the formation of these at first unexpected structures.

For a Li coverage $\theta \leq 0.4$ every Li atom occupies a substitutional site[9,10,19] and the surface exhibits the (2×1) structure in the range $0.2 \leq \theta \leq 0.4$. This substitutional site for $\theta \leq 0.4$ is the same as that of substitutional Li atoms in the (3×3) and (4×4). For $\theta \geq 0.4$ the missing-row structure converts to the (3×3) and then the (4×4) structure to accommodate more Li atoms as adatoms. Adatoms are energetically less favorable than substitutional atoms,[20] but the substitutional sites are already all taken in the (2×1) structure. Therefore, additional Li atoms tend to become adatoms: the coverage of adatoms increases from 0 to 0.111 to 0.25, from (2×1) to (3×3) to (4×4), respectively, while the coverage of substitutional atoms remains almost constant, namely, 0.4, 0.444, and 0.375, respectively. Thus, the average adsorption energy decreases as the coverage increases. It should be noted that surface Cu atoms move around to form small Cu islands for Li adatoms at the conversions from the (2×1) to the (3×3) and from the (3×3) to the (4×4).

One might expect that a (5×5) or other structure could follow the (4×4) at higher coverages. However, the LEED pattern becomes disordered.[10] The reason could be that various local structures become energetically almost equivalent at higher coverages.

In the present study we have demonstrated the power of our symmetrized LEED codes to analyze very complex structures with large unit cells. The symmetrization, which is the major advance over previous versions of our codes, re-

duced the computing times by factors of 100 and 10, respectively, for the reference structure calculation (the most time-consuming step) and the optimization. The memory requirements were also cut, respectively, by factors of 20 and $\frac{5}{4}$. The (4×4) unit cell is the largest among completely determined surface structures by any technique.

In conclusion, we have determined the complex (4×4) structure formed on Cu(001) by Li deposition at 300 K with a symmetrized automated tensor LEED analysis. In this adsorption system, the surface structure changes like $(2\times1)\rightarrow(3\times3)\rightarrow(4\times4)$ with increasing Li coverage. All these structures have now been determined. The (4×4) structure is similar to the (3×3), and can accommodate more Li atoms. It is found that at each Li coverage the Cu(001) surface reconstructs to form a hybrid structure providing the largest adsorption energy.

This work was performed under a Japan-U.S.A. collaboration program supported by JSPS and NSF. This work was partially supported by a grant-in-aid (No. 06452038) for Scientific Research from the Ministry of Education, Science and Culture of Japan, and also supported in part by the Director, Office of Energy Research, Office of Basic Energy Sciences, Materials Sciences Division of the U.S. Department of Energy under Contract No. DE-AC03-76SF00098.

---

*Author to whom all correspondence should be addressed. FAX: +81-11-706-2916. Electronic address: G13787@SINET.AD.JP

†Present address: FEA Inc., 2484 Shattuck Ave., Suite 225, Berkeley, CA 94704-2029.

[1] S. Mizuno, H. Tochihara, A. Barbieri, and M. A. Van Hove, Phys. Rev. B **51**, 1969 (1995).

[2] S. Mizuno, H. Tochihara, A. Barbieri, and M. A. Van Hove, Phys. Rev. B **51**, 7981 (1995).

[3] C. Stampfl and M. Scheffler, Surf. Sci. Lett. **319**, L23 (1994).

[4] J. Burchhardt *et al.*, Phys. Rev. Lett. **74**, 1617 (1995).

[5] H. Brune, J. Wintterlin, R. J. Behm, and G. Ertl, Phys. Rev. B **51**, 13 592 (1995).

[6] K. M. Ho, C. T. Chan, and K. P. Bohnen, Phys. Rev. B **40**, 9978 (1989).

[7] J. V. Barth, R. Schuster, J. Wintterlin, R. J. Behm, and G. Ertl, Phys. Rev. B **51**, 4402 (1995).

[8] J. V. Barth, H. Brune, R. Schuster, G. Ertl, and R. J. Behm, Surf. Sci. Lett. **292**, L769 (1993).

[9] S. Mizuno, H. Tochihara, and T. Kawamura, Surf. Sci. Lett. **292**, L811 (1993).

[10] H. Tochihara and S. Mizuno, Surf. Sci. **279**, 89 (1992).

[11] C. Stampfl, M. Scheffler, H. Over, J. Burchhardt, M. Nielsen, D. L. Adams, and W. Moritz, Phys. Rev. Lett. **69**, 1532 (1992).

[12] J. N. Andersen, M. Qvarford, R. Nyholm, J. F. van Acker, and E. Lundgren, Phys. Rev. Lett. **68**, 94 (1992).

[13] For a review of tensor LEED, see M. A. Van Hove, W. Moritz, H. Over, P. J. Rous, A. Wander, A. Barbieri, N. Materer, U. Starke, and G. A. Somorjai, Surf. Sci. Rep. **19**, 191 (1993).

[14] S. Mizuno, H. Tochihara, and T. Kawamura, Surf. Sci. **293**, 239 (1993).

[15] We have also used the R_2 factor, but we obtained similar results.

[16] J. B. Pendry, J. Phys. C **13**, 937 (1980).

[17] S. Mizuno, H. Tochihara, Y. Matsumoto, and K. Tanaka (unpublished).

[18] L. Pauling, *The Nature of the Chemical Bond*, 3rd ed. (Cornell University Press, Ithaca, 1960).

[19] H. Tochihara and S. Mizuno, Surf. Sci. **287/288**, 423 (1993).

[20] J. Neugebauer and M. Scheffler, Phys. Rev. B **46**, 16 067 (1992).

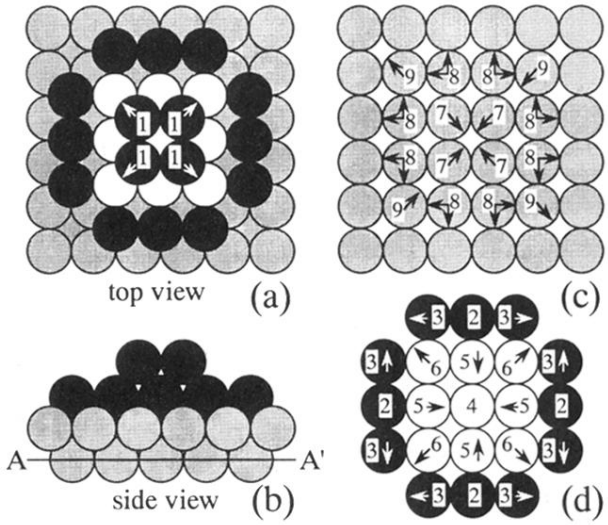

FIG. 3. (a) Top and (b) side views of the best-fit Cu(001)-(4×4)-10Li structure (model 18 in Fig. 1). Dark-gray spheres are Li atoms, light-gray spheres represent Cu atoms in the complete Cu layers, while blank spheres are Cu atoms in the mixed layer. The numbers identify symmetrically equivalent atoms. Arrows indicate directions of displacements from ideal hollow sites. The line *A*-*A'* in the side view is the base line for heights shown in Table I. (c) Top view of the first complete Cu(001) layer. (d) Top view of the mixed layer.